Advances in Science and Technology Research Journal, 2026, 20(1), 162–182 https://doi.org/10.12913/22998624/210942 ISSN 2299-8624, License CC-BY 4.0 Received: 2025.08.25 Accepted: 2025.09.26 Published: 2025.11.21

Experimental analysis of process parameters in micro-milling of AA6063-T6 using 7% cobalt WC tools

Vipul Prabhakar Rathod^{1,2,3*}, Sandeep Haribhau Wankhade^{1,3}, Yogesh Ganpat Kamble^{2,3}

- ¹ Department of Mechanical Engineering, AISSMS COE, Pune Maharashtra, 411001, India
- ² Department of Robotics and Automation Engineering, D Y Patil College of Engineering, Akurdi Pune Maharashtra, 411044, India
- ³ Savitribai Phule Pune University, Pune, 411007, India
- * Corresponding author's e-mail: rvipul69@gmail.com

ABSTRACT

Recent advancements in ultra-precision machining center have significantly enhanced the capability to produce high-quality aluminium alloy components with improved accuracy, superior surface finish, and extended tool life. The growing demand for precision-manufactured aluminium parts in industries such as aerospace, automotive, biomedical devices, and electronics has increased the need for optimized machining strategies. This study examines the influence of various machining parameters on key performance measures, including surface integrity, dimensional accuracy, and tool wear, during the machining of aluminium alloys. A definitive screening design (DSD) experimental methodology is employed to efficiently evaluate multiple process variables and their interactions while minimizing the number of experimental trials. This approach facilitates the identification of the most significant parameters affecting machining performance, enabling data-driven optimization of the process. This study investigates the micro-milling performance of uncoated WC tools with 7% cobalt binder, unlike conventional 11% cobalt tools, as a suitable choice for machining softer aluminium alloys. The work uniquely integrates experimental trials with ANOVA-based statistical analysis to capture the influence of spindle speed, feed rate, and depth of cut on cutting forces and surface roughness. The findings provide process-level insights and evidence based guidelines for optimizing micro-milling of AA6063-T6. The study highlights that spindle speed is the most critical parameter, contributing nearly half of the performance variations, with optimized settings achieving superior surface finish of 0.0384 μm and reduced cutting forces, thereby extending tool life and ensuring stable, highquality micro-milling of AA6063-T6 (ASTM).

Keywords: micro-manufacturing, micro milling, ultra-precision machining, surface quality.

INTRODUCTION

Micro-milling is a precision machining process capable of producing extremely fine features and high-quality surface finishes using cutting tools with diameters typically smaller than 1 mm. It offers a unique combination of high material removal rates and exceptional dimensional accuracy, making it indispensable for industries such as aerospace, medical devices, and microelectronics, where miniature components must meet stringent performance and quality standards. The

rapid development of ultra-precision, high-speed machining center has expanded the scope of micro-milling, enabling the creation of complex geometries on a wide range of materials.

Among the factors that determine process performance, the selection of tool material is critical. Tungsten carbide (WC) is widely used due to its high hardness, resistance to wear, and ability to retain sharp cutting edges even under elevated temperatures. However, when machining aluminium alloys, challenges such as built-up edge (BUE) formation can occur. BUE results from

adhesion of the workpiece material to the cutting edge, caused by heat generated through friction and material shearing. This leads to uneven wear, increased cutting forces, and compromised surface quality. To overcome these limitations, solutions such as advanced tool coatings and cryogenic treatments are often applied, improving heat dissipation, reducing adhesion, and enhancing tool life. The insights presented in this work aim to deepen the understanding of micro-milling behavior when machining aluminium alloys, highlighting key process challenges, their root causes, and strategies for achieving improved productivity, tool longevity, and consistent surface integrity in high-precision manufacturing.

Across metals and alloys, micro-machining performance emerges from a tight interplay of cutting parameters, coatings, and thermo-mechanical treatments, with recurring trade-offs between productivity, surface integrity, and tool life [1]. In aluminum systems, increasing feed rate (FR) and depth of cut (DOC) boosts material removal rate (MRR) in AA6063 T6, though higher FR/DOC and spindle speed (SS) threaten stability and dimensional accuracy, underscoring the need for balanced settings [2]. The experiments on micro-milling of aluminum alloys showed that when spindle speed was increased, the thrust force dropped by nearly 20-25%, reducing tool load and improving machining stability. At the same time, increasing the feed rate and depth of cut caused the cutting forces to rise by about 15-30%, which also led to faster tool wear. Comparing tool geometries, sharper tools reduced cutting forces by almost 10-15% and produced surfaces that were about 20% smoother. Overall, the study found that using higher spindle speeds with optimized tool angles could extend tool life by more than 25% while significantly improving surface quality, proving that parameter optimization directly boosts efficiency and reliability in micromilling [3].

For AA6061 T6 micro-channels, higher spindle speed and depth of cut tend to lower surface roughness but aggravate burr width, while reducing feed improves burr control yet risks rougher finishes; optimization must therefore treat input parameters as coupled levers rather than independent knobs [4, 5]. Geometry control at the micro-scale is further complicated by runout: in AA1100 impeller work, measured minimum thickness diverged from target because runout inflated effective chip thickness, directly degrading

dimensional fidelity despite high-speed, dry TiAlN tooling [6]. Additively manufactured AlSi alloys amplify these sensitivities: AlSi10Mg's higher Si content elevates forces (Fx, Fy, Fz) and roughness relative to AlSi7Mg; although raising SS generally helps Ra, it also increases cutting forces due to oxide/SiO2 fragments, making feed reduction and conservative DOC essential for force containment [7, 8]. In nickel-rich alloys, coating choice and thermal management dominate outcomes: on Inconel, PECVD DLC increases edge hardness and lowers friction, suppressing BUE, flank wear, and burrs while improving Ra and force levels across feeds and shallow DOCs [9]; on Inconel 718, cryogenic pre-cooling and MQL both curb BUE/adhesion and tool wear with cryogenic often yielding the best Ra and burr suppression, while MQL's temperature stabilization indirectly reduces burrs via wear mitigation [12, 13]. Coating effects are nuanced: TiSiN often delivers the lowest Ra in both Monel 400 and Inconel 718 by raising interfacial temperature through higher friction to ease shearing, yet it can elongate top burrs under certain edge/cutting-force regimes; nACo's high hardness elevates forces and roughness and promotes BUE on Inconel 718 [10]; AlTiN, by contrast, tends to restrain topburr formation in 718 compared to TiSiN [11]. Difficult-to-cut titanium alloys echo similar patterns: AlTiN-coated micro end mills resist wear and preserve edge geometry, maintaining lower Ra over long cutting lengths versus uncoated/Al-CrN/TiN peers [14, 15]; amorphous-carbon coatings markedly cut forces and roughness but face debonding risks as feed and cutting length rise; adding WS₂ as a solid lubricant to TiAlN slashes forces (Fx \sim 60%, Fy \sim 70%) and wear, although the same addition to TiAlSiN does not replicate the benefit highlighting the coating-substrateedge-radius triad as decisive in net performance [16–18]. Beyond coatings, deep cryogenic treatment (DCT) of WC-Co end mills (and cryogenic variants applied to coated carbides) refines grains, strengthens Co–WC bonding, promotes η-carbide phases, and lifts microhardness (~9-11%), which translates to lower forces, reduced BUE, and extended life in Ti-6Al-4V and AISI steels; sub-zero treatments can help, but DCT-24 h repeatedly emerges as the best performer, with wear and surface roughness improvements most pronounced at feeds that otherwise excite abrasion/adhesion modes [19, 20]. Differential Carbide Treatment subtly increases the harder ε-Co phase especially

at high cobalt contents (e.g., WC-80Co), offering incremental hardness/wear gains and suggesting composition-dependent benefits for microtools that run near stability limits [21]. Process environment and material pairing still matter: for medical-grade channels, 316L benefits from coolant (more rectangular, stable channels and best surface roughness), whereas Ti6Al4V often prefers dry or low-speed/wet combinations depending on depth targets; in both cases, FR and cooling jointly govern achievable geometric fidelity and depth control [22]. Wear evolution in stainless micro-milling tracks a three-phase path - from slight edge rounding to chipping to severe fracture with cutting forces rising from ~2.45 N to ~4.93 N; sharp edges wear faster by chipping, and machine-learning models (Random Forest) trained on force and geometry signals can forecast remaining life, enabling preemptive tool change before catastrophic loss [23, 24]. Drilling microholes in titanium further shows that tool diameter and feed dominate survivable hole count: higher feeds and larger diameters lift AE RMS/ASL via friction and contact length, accelerating failure and reducing hole yield, so optimal windows skew toward moderate diameters, higher speeds, and restrained feeds [25, 26]. Even in comparatively free-cutting brass, tool state drives mechanics: worn tools (smaller effective diameter, more negative rake) amplify forces and roughness, with FR consistently raising force in both up- and down-milling while speed tends to lower it; roughness trends invert with strategy (downmilling roughness increases with feed, up-milling decreases with higher feed/speed), reminding that kinematics and edge geometry must be co-tuned [25]. Finally, across Monel/Al alloys, burrs are minimized at moderate SS and DOC with midrange feeds, but local geometry (e.g., Y-junctions, curvature) can flip the feed-burr relationship by altering chip flow and ploughing propensity, making channel-type-specific optimization necessary [10, 27]. Together, these studies argue for a holistic recipe: select coatings/treatments to set the thermal-tribological envelope (DLC, AlTiN, TiSiN, WS₂, DCT) [25]; stabilize the mechanics with conservative edge radii, verified runout, and appropriate cooling/MQL/cryogenics [24]; and then dial SS/FR/DOC within material-specific windows to trade MRR against force, burrs, and surface roughness ideally closed-looped by force/ AE sensing and predictive models to keep the process inside a wear-savvy stability basin [26].

The review explains how different treatments for tungsten carbide micro-tools affect micromilling of aluminium alloys. It shows that untreated tools are cheap but wear out quickly, coated tools last longer and give better surface quality but can fail under stress, and cryogenically treated tools are the most durable, staying sharp and stable while also being more sustainable. It suggests that combining coatings with cryogenic treatment could deliver the best results, helping industries achieve more precise, efficient, and eco-friendly micro-milling operations [24]. Tungsten carbide tools are commonly used, but they wear out fast unless enhanced with cryogenic cooling (deep freezing) or special coatings like TiN, TiAlN, or DLC [25]. These treatments make tools stronger, last longer, and produce smoother surfaces. The study also highlights how machining settings like spindle speed, feed rate, and depth of cut-affect performance, and how advanced high-speed machines boost accuracy and efficiency. It concludes by stressing the need for future research on new coatings, hybrid processes, smart monitoring, and eco-friendly practices to make micro-milling even more precise, costeffective, and sustainable [26, 27].

The review makes it clear that successful micro-milling depends on carefully balancing tool materials, surface treatments, and cutting parameters to meet the competing demands of accuracy, productivity, and tool life. While untreated tools remain cost-effective, they wear rapidly, making coatings and cryogenic treatments essential for long-term reliability and smoother surfaces. Coated tools, especially with advanced films like AlTiN or DLC, can extend tool life and improve finish, though they sometimes face limitations under extreme conditions. Cryogenic treatment, on the other hand, consistently enhances hardness and stability, often outperforming conventional tools. The evidence also suggests that hybrid approaches combining coatings with cryogenic treatment hold strong promise for future industrial applications by improving precision, efficiency, and sustainability at the same time. Alongside tool improvements, the right choice of spindle speed, feed rate, and depth of cut remains crucial, since these settings directly affect forces, burr formation, and surface quality. Overall, the findings highlight that optimized combinations of advanced tool treatments and parameter control can push micro-milling toward greater accuracy, durability, and eco-friendly performance, while future

research should focus on hybrid solutions, smart monitoring, and sustainable machining strategies. The novelty of this study lies in presenting an integrated experimental and statistical analysis of uncoated WC tools in micro-milling of AA6063-T6, bridging the gap between empirical data and predictive understanding of process behaviour. The selection of a tungsten carbide tool with 7% cobalt binder content instead of the conventional 11%. Since the experiments were carried out on a softer material like aluminium alloy, a lower cobalt percentage was preferred to enhance hardness and wear resistance of the tool while minimizing unnecessary toughness, thereby improving machining performance and tool life. Unlike existing studies that primarily focus on coated or cryogenically treated tools, this work isolates the fundamental influence of spindle speed, feed rate, and depth of cut on surface roughness and cutting forces using ANOVA-driven insights. By systematically quantifying the parameter sensitivities, this research offers evidence-based guidelines for optimizing micro-milling operations.

EXPERIMENTAL SETUP

The micro-milling experiments were carried out on a high-precision, multi-axis machine specifically designed for micromachining hardto-cut materials such as tool steels, titanium alloys, and nickel-based superalloys. The X and Y axes each offer a 100 mm travel range, driven by precision ground ball screws and brushless DC servomotors, supporting feed rates from as low as 0.06 mm/min up to 6000 mm/min. These axes can handle loads of up to 25 kg horizontally and 10 kg in vertical and sideways directions, with a resolution of 0.5 microns to ensure precise tool positioning during fine machining operations. The Z-axis is engineered for ultra-high precision, featuring a frictionless, pneumatically counterbalanced mechanism and a non-contact directdrive brushless linear motor. It offers a 60 mm travel range, the same feed rate range as the X and Y axes, and supports vertical loads up to 10 kg. With a resolution as fine as 1 nanometer and accuracy within ± 0.3 microns, the Z-axis allows for highly controlled depth adjustments during micro-milling or drilling. The spindle is capable of ultra-high speeds ranging from 5,000 to 170,000 rpm, driven by a variable frequency drive and using a Mega 4S collet system with just 1 micron

of runout. It supports tools with a 3 mm shank diameter and provides approximately 5.6 N-cm of torque, making it suitable for both milling and drilling at the microscale. The machine's frame is constructed from high-damping granite, which offers excellent thermal stability and minimizes vibration, enhancing overall surface quality. Its Z-stage is optimized for nano-level accuracy, while the X and Y stages employ cost-effective, high-stiffness ceramic bearings. Altogether, this setup combines high spindle speeds, accurate feed control, and a rigid, thermally stable structure ideal for precision micromachining of challenging materials with surface roughness values reaching as low as ~100 nm. Figure 1 shows the experimental setup consisting of the spindle and tool holder, the workpiece mounted on the dynamometer for measuring cutting forces.

Tool and workpiece

A 500-micron (0.5 mm) micro end mill is a highly precise cutting tool designed for machining extremely small and intricate features. At this miniature scale, the performance of the tool is heavily dependent on the choice of material, as even the slightest wear, deformation, or change in edge geometry can lead to significant deviations in dimensional accuracy and surface finish. WC

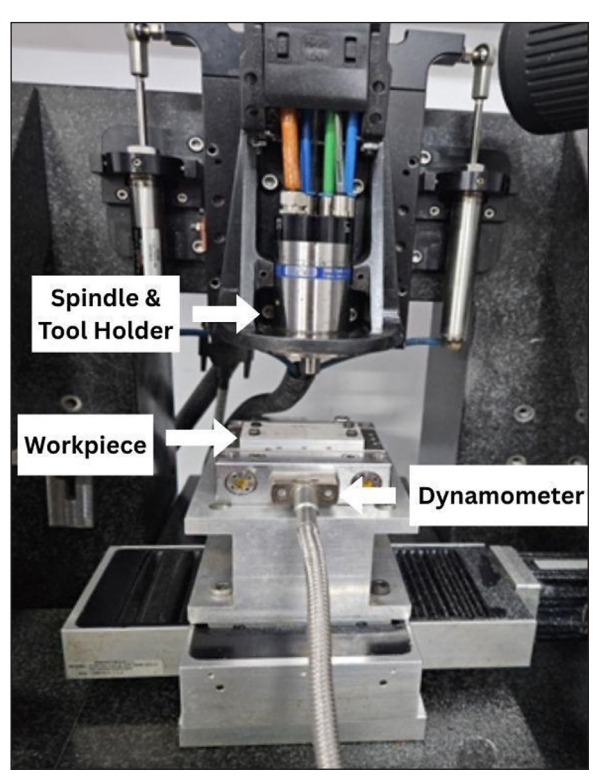


Figure 1. Experimental setup

is the most widely adopted material for such applications because it offers a rare combination of extreme hardness, high wear resistance, and the ability to maintain a sharp cutting edge under demanding machining conditions.

Tungsten carbide is produced by combining tungsten and carbon particles with a metallic binder, typically cobalt, through a sintering process. This creates a dense and exceptionally hard material, with hardness values approaching those of diamond (8.5–9.0 on the Mohs scale). Its high hardness enables the cutting edges to resist abrasion from the workpiece material, even under high cutting speeds and feed rates. Furthermore, tungsten carbide's high compressive strength allows it to withstand the intense mechanical stresses encountered during precision machining without chipping or breaking, which is particularly important for micro tools with very fine geometries.

Another key reason for choosing tungsten carbide is its high thermal conductivity. During machining, especially at high spindle speeds, substantial heat is generated from both friction and the shearing of material in the cutting zone. This heat can soften cutting edges, cause thermal deformation, and reduce tool life. Tungsten carbide efficiently dissipates this heat away from the cutting edge, reducing thermal stress and helping maintain dimensional stability throughout the machining process.

In micro end mills, the cobalt content in WC tools greatly influences performance. 7% Co WC

tools have higher hardness and wear resistance, making them ideal for achieving better surface finish and precision in micro milling of aluminium alloys like 6063-T6. However, they are more brittle and prone to chipping under high loads. On the other hand, 11% Co WC tools offer greater toughness and resistance to fracture, making them suitable for roughing cuts, higher feed rates, and vibration-prone conditions, though they have slightly lower wear resistance and may produce a less refined finish. In practice, 7% Co tools are preferred for finishing, while 11% Co tools are more reliable for roughing or demanding operations. Figure 2 shows the micro machining operation captured using a high-speed camera, where a 500-micron end mill tool is machining AA 6063 T6, producing a micro-milled surface (Table 1).

When machining aluminium alloys, additional challenges such as BUE formation can occur. BUE happens when small fragments of workpiece material adhere to the cutting edge due to the combined effects of friction, pressure, and heat. This not only alters the cutting geometry but also increases cutting forces, accelerates tool wear, and degrades surface finish quality. Although tungsten carbide's hardness and thermal stability help to mitigate these issues, they do not eliminate them entirely. For this reason, advanced strategies such as applying protective tool coatings or using cryogenic treatments are often employed. Coatings can reduce friction and adhesion, while cryogenic cooling can help maintain

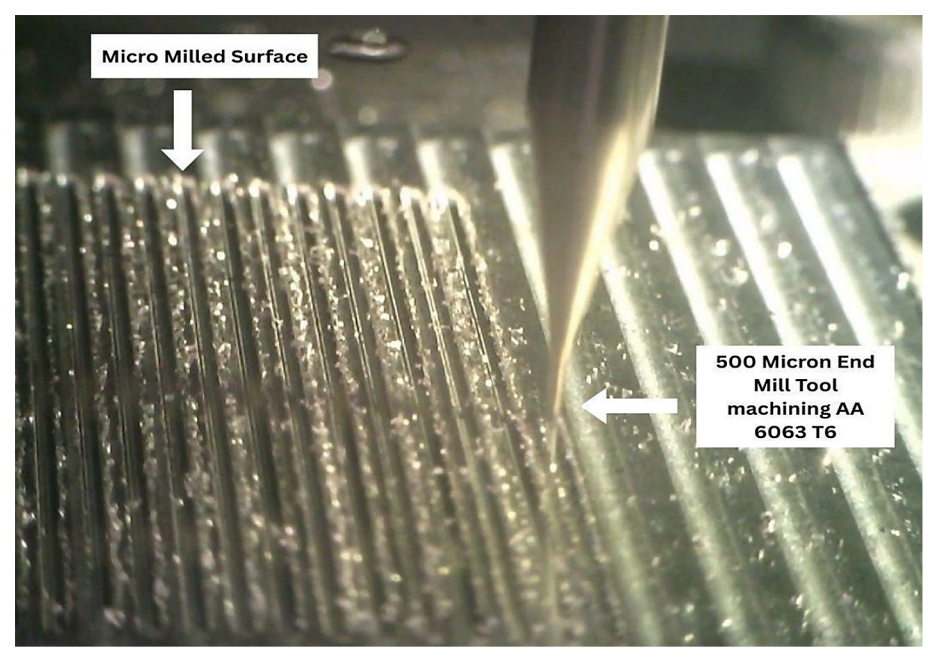


Figure 2. Micro machining operation captured using high speed camera

Table 1. Composition of tungsten carbide micro end mill tool

Element	W	Со	Р	Cr	Sc	Gd	Ge	S	Fe	Ca
Percentage (%)	89.9	6.69	0.63	0.73	0.2	0.48	0.7	0.24	0.21	0.21

Table 2. Composition of aluminium Alloy 6063 T6

Name of the element	Al	Mn	Si	Cu	Zn	Ti	Fe	Mg
Weight percentage (%)	98.63	0.034	0.349	0.084	0.085	0.034	0.134	0.594

lower cutting temperatures, both of which extend tool life and improve performance (Table 2).

Figure 3 shows the methodology adopted for the experiment using definitive screening design (DSD), where a 500-micron WC end mill tool was used to machine Aluminium Alloy 6063 T6, with cutting forces measured by a Kistler Mini-Dyn dynamometer and surface roughness evaluated using a Bruker Alicona Micro CMM.

DESIGN OF EXPERIMENT

In the present study, the input process parameters spindle speed, feed rate, and depth of cut were selected based on a DSD approach. This design method is particularly useful for efficiently identifying the most influential factors in a process while minimizing the number of experimental runs. The chosen levels for each parameter represent practical extremes and midpoints, ensuring that both linear and potential curvature effects can be evaluated.

For micro milling, the spindle speed range (15,000–35,000 rpm) covers the typical operational limits for ultra-high-speed machining of miniature features, where cutting forces and heat generation must be carefully controlled. The feed rate range (3–7 mm/min) was selected to capture both low and high material removal rates, which

directly influence tool engagement, surface quality, and burr formation. The depth of cut range (40–60 μ m) was kept in the micro-scale to avoid excessive tool loading while allowing measurable variations in cutting forces and surface finish.

In a DSD, each factor is run at three levels allowing the model to detect not only main effects but also quadratic and some interaction effects without requiring a full factorial design. In the context of micro milling, this approach ensures that the relationships between process parameters and critical responses such as surface roughness, cutting forces, and dimensional accuracy can be understood with high efficiency and minimal resource usage (Table 3).

RESULTS AND DISCUSSION

In ANOVA analysis, several key terms help explain how each factor influences the results. Contribution shows the percentage share of how much a particular factor, such as spindle speed or feed rate, affects the outcome, helping identify which parameters are most influential. Adjusted Sum of Squares (Adj SS) represents the amount of variation explained by that factor after accounting for the effects of other parameters, showing its unique impact. Adjusted Mean Square (Adj MS) takes this further by averaging the variation per

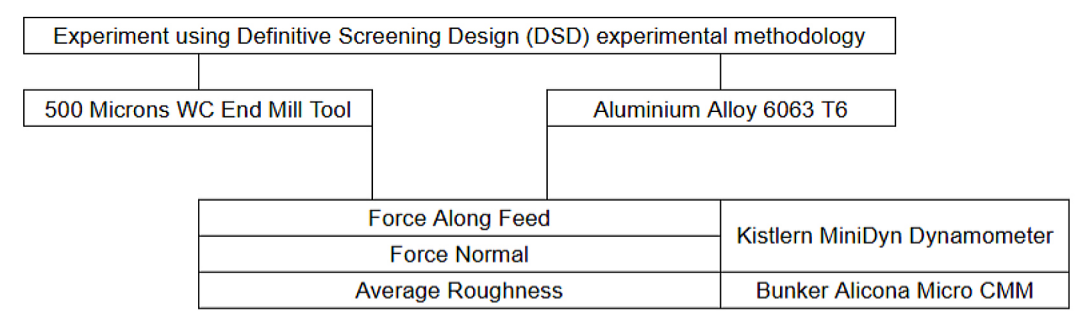


Figure 3. Methodology

Table 3. Design of experiment

Input parameters	Spindle speed (RPM)	Feed rate (Microns/Flute)	Depth of cut (Microns)
Low	15000	3	40
Moderate	25000	5	50
High	35000	7	60

level of the factor, indicating how consistently it affects the response. The F-value acts like a signal-to-noise ratio, comparing the effect of the factor to random experimental noise, where a higher value means the factor has a stronger and more reliable influence. Finally, the P-value indicates the probability that the observed effect is due to chance; a value below 0.05 typically signals that the factor is statistically significant and genuinely affects the outcome. Together, these metrics make it easier to understand which parameters matter most and how confidently their effects can be trusted in a machining or micro-milling study.

FORCE ALONG FEED

The ANOVA Table 4 presents the statistical analysis of three input parameters on the response. Among these, feed rate (FR) shows the most significant influence, contributing approximately 35.51% to the overall variation with a P-value of 0.003, indicating a highly significant effect. Spindle speed (SS) also plays a strong

role, contributing 28.65%, and is statistically significant with a P-value of 0.006. DOC contributes 15.36% with a P-value of 0.029, meaning it has a noticeable, though smaller, impact. The overall model's R-squared value is 89.52%, suggesting the model is highly reliable. Figure 4 shows the variation of cutting forces along the feed direction (Fx) and normal direction (Fy) with time, highlighting the machining start, steady-state cutting, and machining end.

Force along feed VS feed rate and spindle speed: Figure 5 and Figure 8, It is found that with an increase in SS, force along feed (FX) decreases, while with an increase in FR, force along feed shows a slight increase. For higher SS and lower FR, less force along feed is observed. This is confirmed in the surface plot, which shows that higher spindle speed and lower feed rate are favorable as they produce lower force along feed, thereby reducing the load on the tool and machine.

Force along feed VS depth of cut and spindle speed: Figure 6 and Figure 9 It is found that with an increase in SS, FX decreases, whereas with an increase in DOC, force along feed increases. For

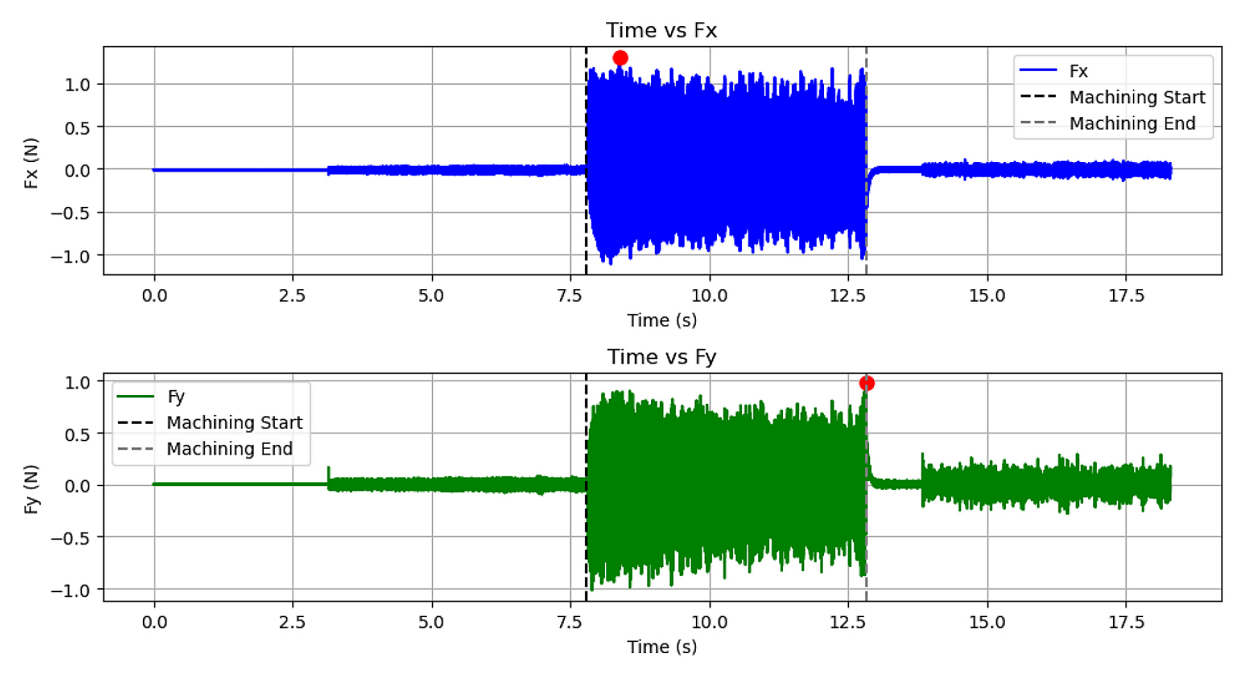


Figure 4. Graphs for force along feed and force normal

Table 4. ANOVA for force along feed

Source	Contribution	Adj SS	Adj MS	F-Value	P-Value
Model	79.52%	2.5426	0.84752	11.65	0.002
Linear	79.52%	2.5426	0.84752	11.65	0.002
SS	28.65%	0.916	0.91598	12.59	0.006
FR	35.51%	1.1354	1.13539	15.61	0.003
DOC	15.36%	0.4912	0.49119	6.75	0.029
Error	20.48%	0.6547	0.07275		
Total	100.00%				
R-Sq	89.52				

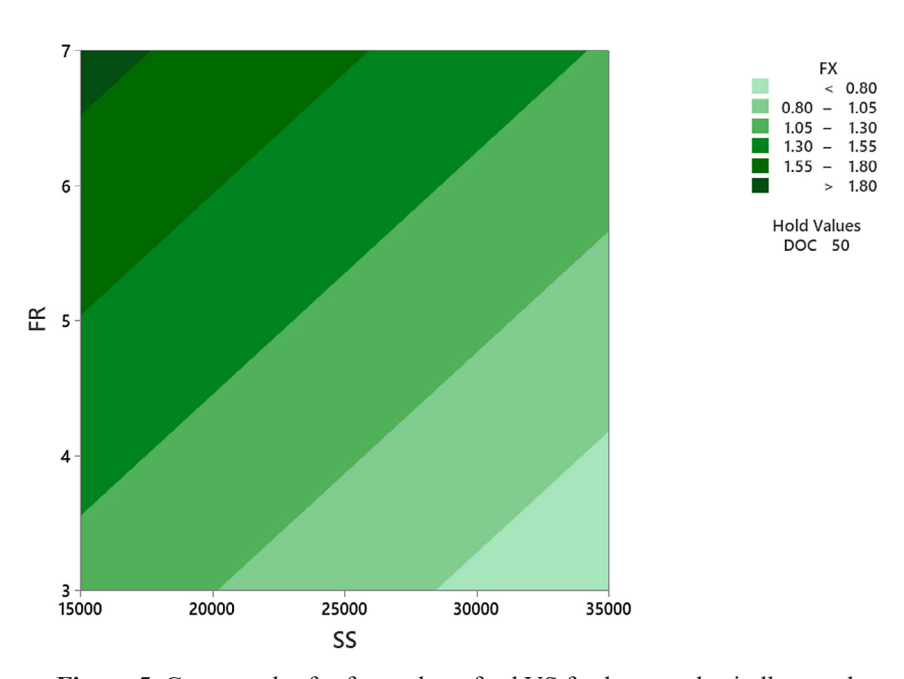


Figure 5. Contour plot for force along feed VS feed rate and spindle speed

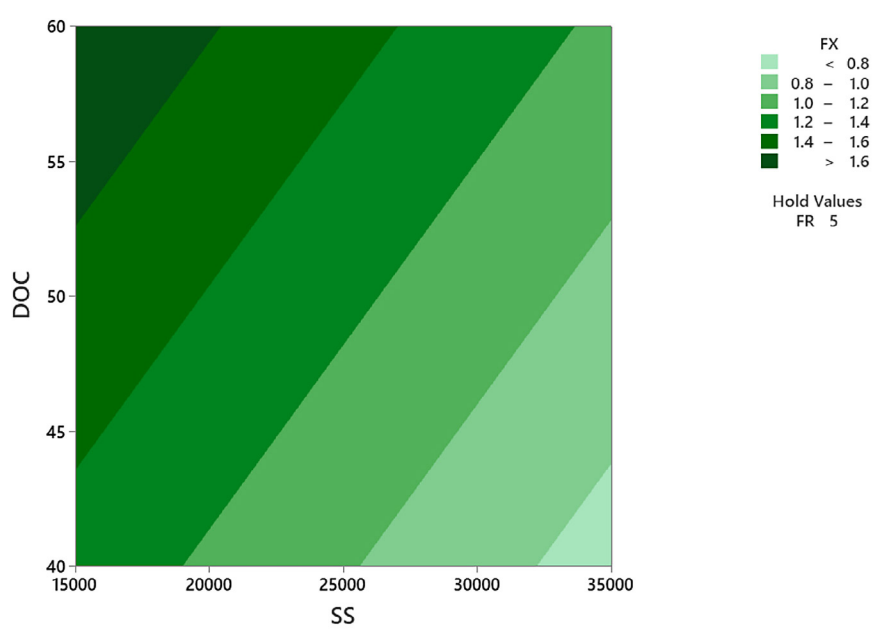


Figure 6. Contour plot for force along feed VS depth of cut and spindle speed

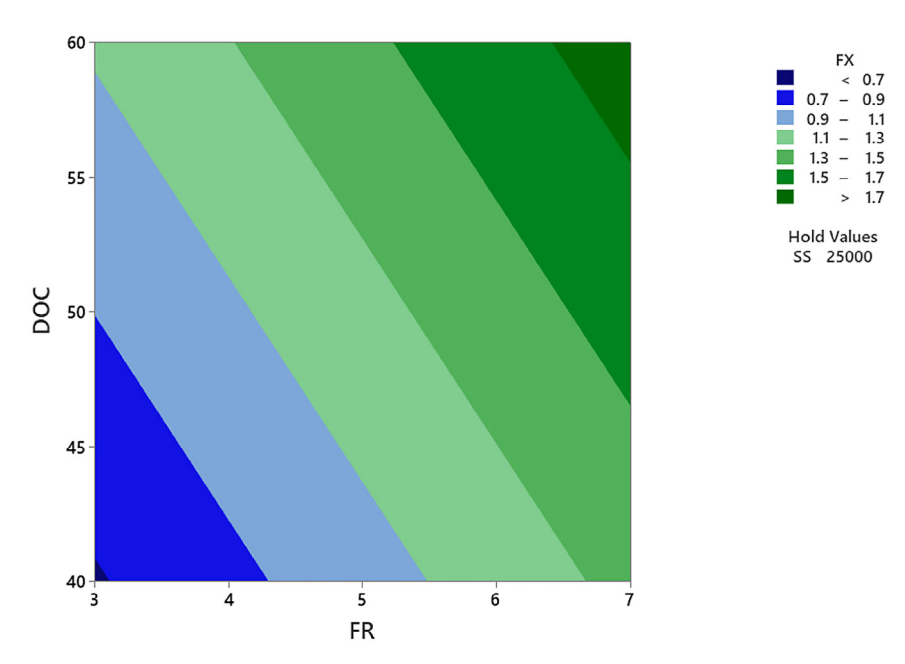


Figure 7. Contour plot for force along feed VS depth of cut and feed rate

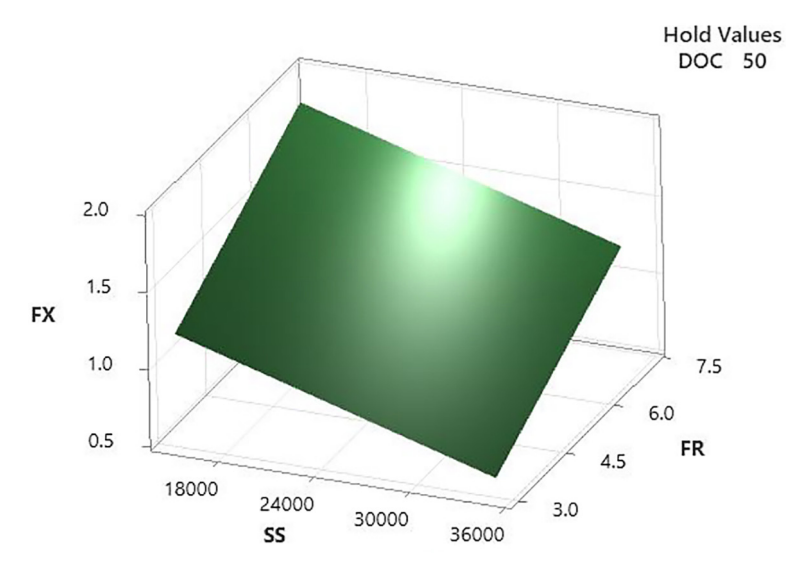


Figure 8. Surface plot for force along feed VS feed rate and spindle speed

higher SS and lower DOC, less force along feed is observed. This is confirmed in the surface plot, which indicates that higher spindle speed combined with a smaller depth of cut is favorable as it produces lower force along feed, resulting in reduced load on the tool and machine.

Force along feed VS Depth of cut and Feed Rate: Figure 7 and Figure 10, It is found that with an increase in feed rate (FR), FX increases, and similarly, with an increase in DOC, force along feed increases. For lower FR and lower DOC, less force along feed is observed. This is confirmed in the surface plot, which shows that maintaining

both feed rate and depth of cut at lower values is favorable as it produces lower force along feed and reduces the load on the tool and machine.

Figure 11 shows For Force along feed, the main effects plot shows that increasing spindle speed from 20,000 to 60,000 RPM causes a clear and steady decrease in force, with the lowest force along feed at the highest speed due to reduced chip load and smoother cutting. Feed rate has a strong positive effect, where increasing from 2 to 6 mm/min significantly raises force along feed because of increased chip thickness and material engagement. Depth of cut also contributes to

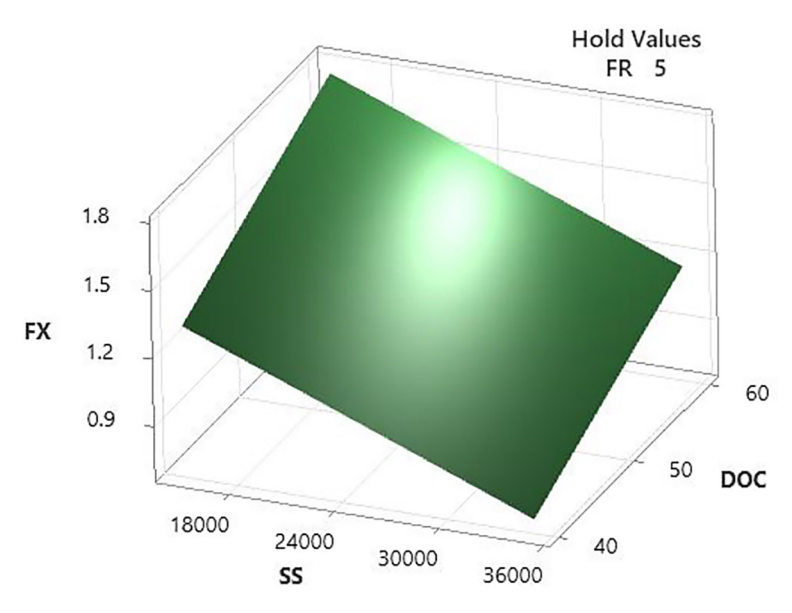


Figure 9. Surface plot for force along feed VS depth of cut and spindle speed

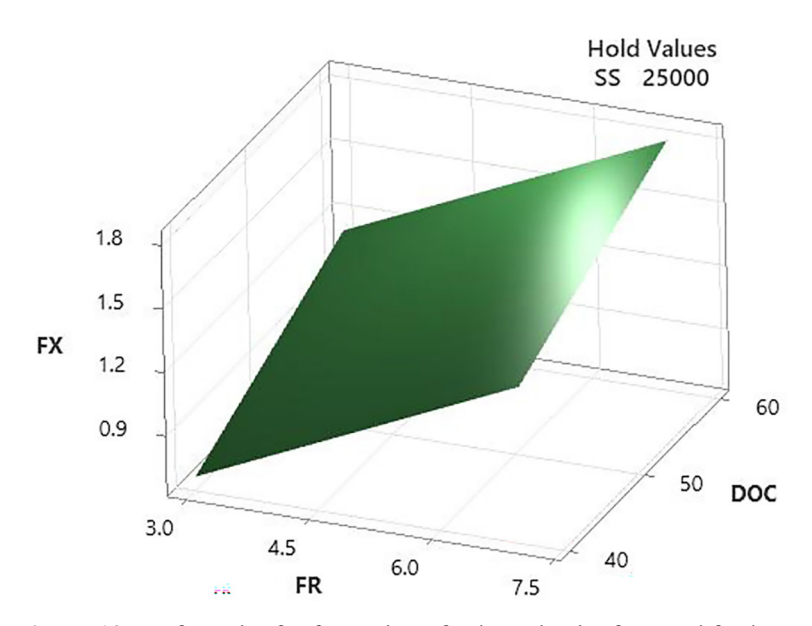


Figure 10. Surface plot for force along feed VS depth of cut and feed rate

higher force along feed values; as DOC increases from 40 to 80 μm , the force rises notably since more material must be sheared per pass. Thus, for minimizing force along feed, high spindle speed, low feed rate, and low DOC are preferable.

FORCE NORMAL

The ANOVA Table 5 presents the statistical analysis of three input parameters on the response. Among these, spindle speed (SS) shows the most significant influence, contributing approximately 39.07% to the overall variation with

a P-value of 0.000, indicating a highly significant effect. FR follows closely, contributing 35.32%, and is statistically significant with a P-value of 0.001. DOC contributes 13.47% with a P-value of 0.012, meaning it has a noticeable but smaller impact. The overall model's R-squared value is 87.86%, indicating it is a strong and reliable fit.

Force normal VS feed rate and spindle speed: Figure 12 and Figure 15, It is found that with an increase in SS, force normal (FY) decreases, while with an increase in FR, force normal increases slightly. For higher SS and lower FR, less force normal is observed. This is confirmed in the surface plot, which shows that higher spindle speed and lower

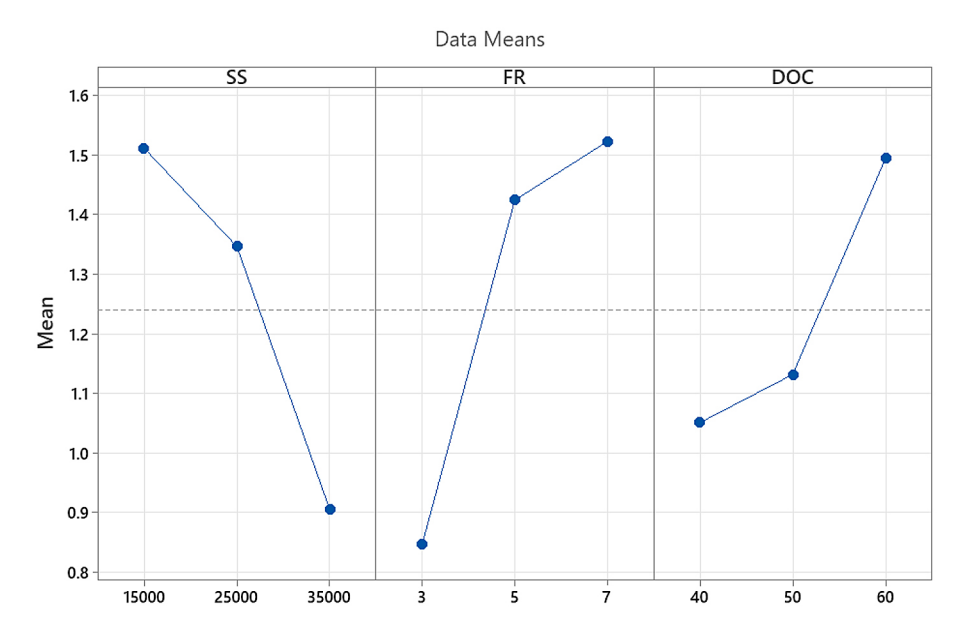


Figure 11. Main effect plot for force along feed

Table 5. ANOVA for force normal

Source	Contribution	Adj SS	Adj MS	F-Value	P-Value
Model	87.86%	2.4082	0.80274	21.72	0
Linear	87.86%	2.4082	0.80274	21.72	0
SS	39.07%	1.0709	1.07093	28.97	0
FR	35.32%	0.9681	0.96814	26.19	0.001
DOC	13.47%	0.3691	0.36914	9.99	0.012
Error	12.14%	0.3327	0.03696		
Total	100.00%				
R-Sq	87.86				

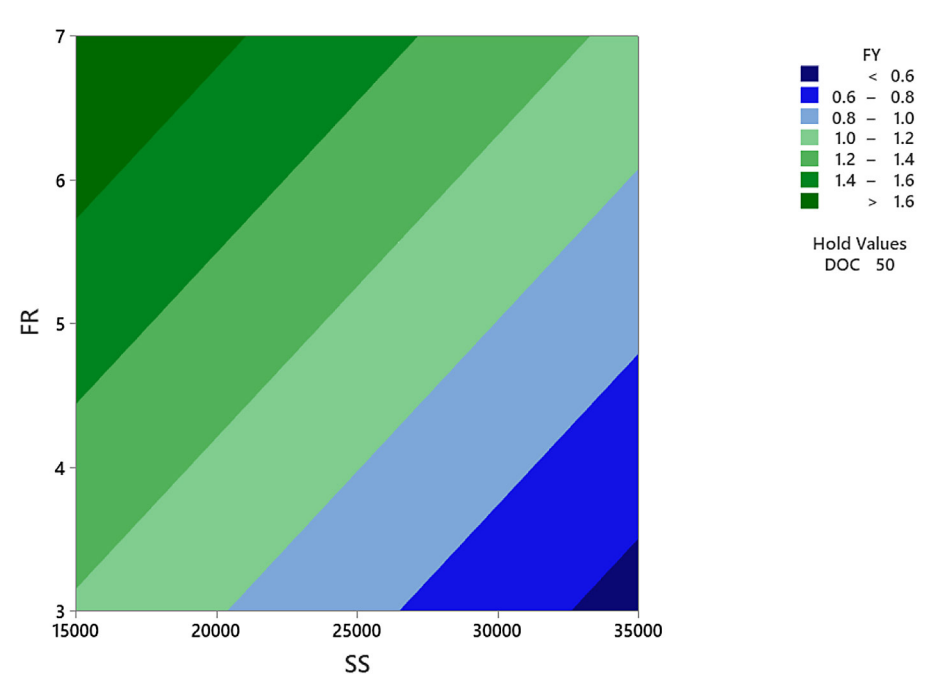


Figure 12. Contour plot for force normal VS feed rate and spindle speed

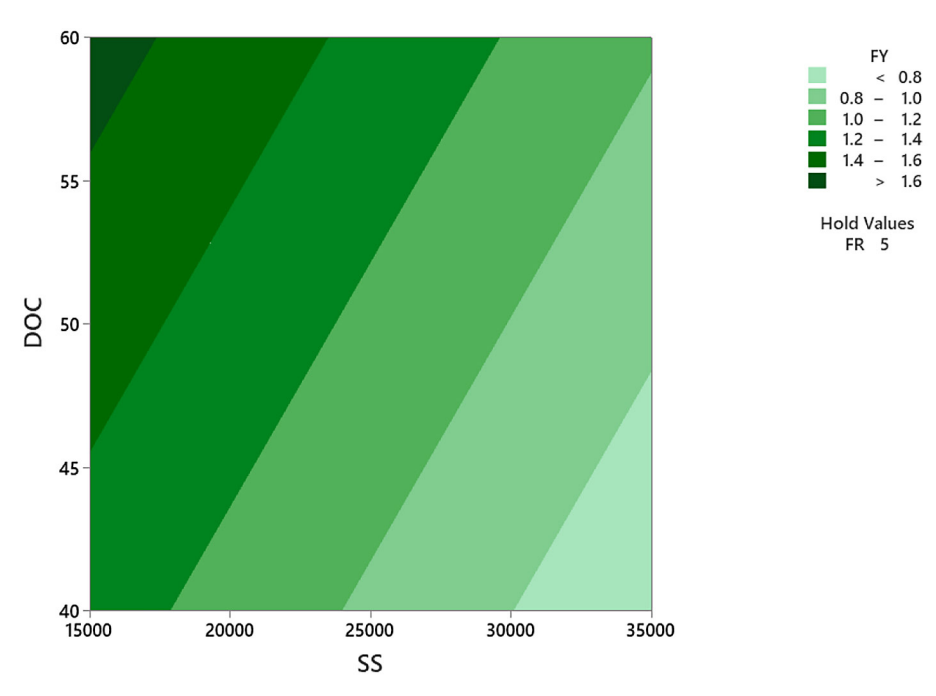


Figure 13. Contour plot for force normal VS depth of cut and spindle speed

feed rate are favorable as they produce lower force normal, resulting in reduced tool and machine load. Force normal VS depth of cut and spindle speed: Figure 13 and Figure 16, It is found that with an increase in spindle speed (SS), force normal (force normal) decreases, whereas with an increase in DOC, force normal increases. For higher SS and lower DOC, less force normal is observed. This is confirmed in the surface plot, which shows

that higher spindle speed and lower depth of cut are favorable as they produce lower force normal, thereby minimizing load on the tool and machine. Force normal VS depth of cut and feed rate: Figure 14 and Figure 17, It is found that with an increase in FR, FY increases, and with an increase in DOC, force normal also increases. For lower FR and lower DOC, less force normal is observed. This is confirmed in the surface plot, which indicates that

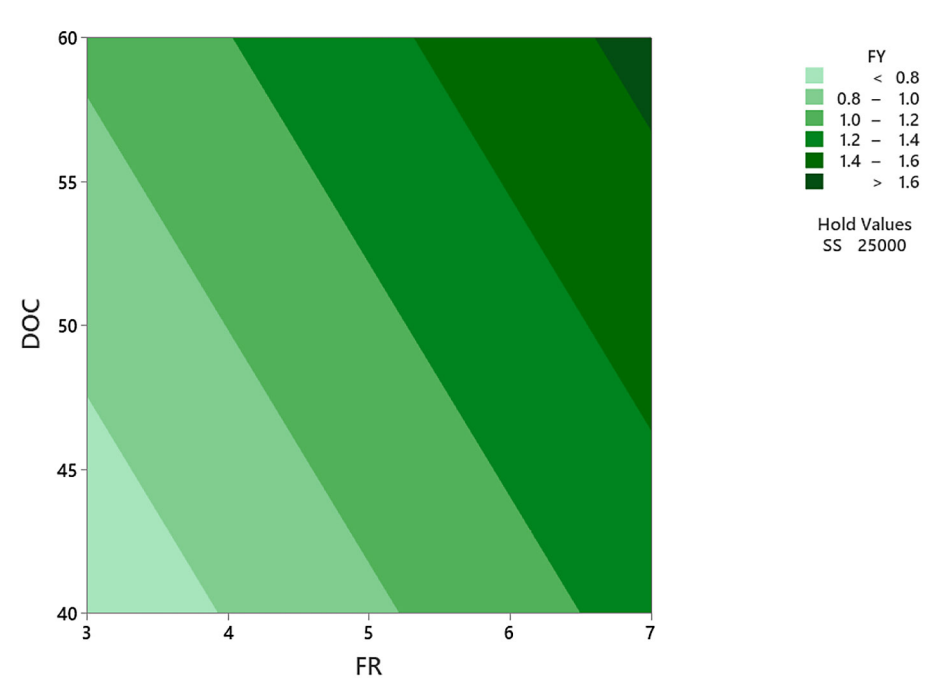


Figure 14. Contour plot for force normal VS depth of cut and feed rate

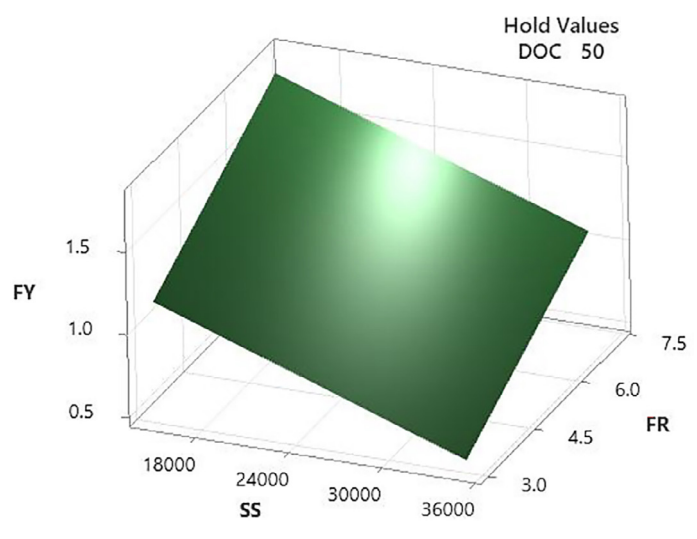


Figure 15. Surface plot for force normal VS feed rate and spindle speed

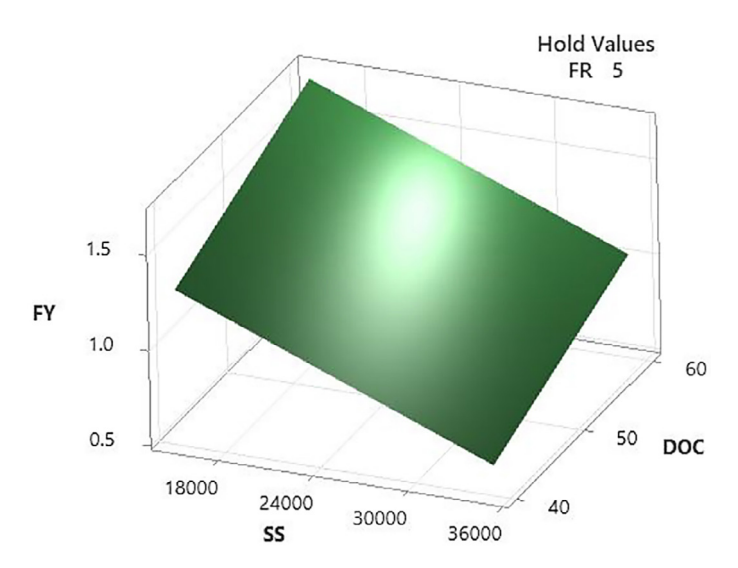


Figure 16. Surface plot for force normal VS depth of cut and spindle speed

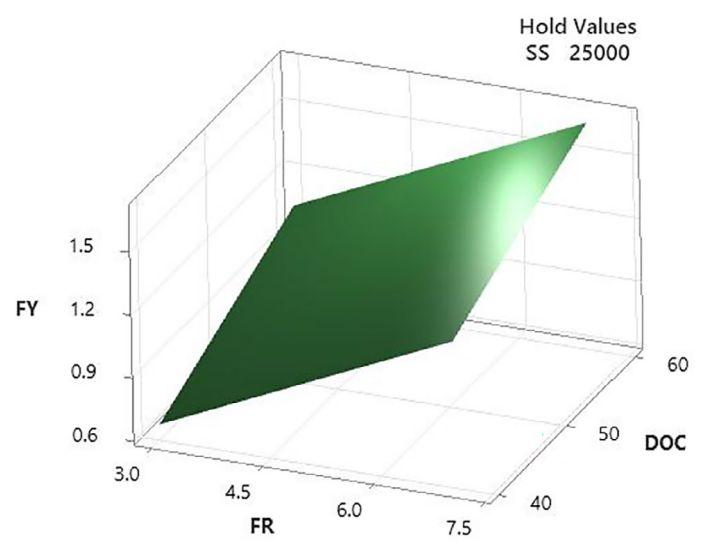


Figure 17. Surface plot for force normal VS depth of cut and feed rate

lower feed rate and lower depth of cut are favorable for producing lower force normal and reducing machine stress. Figure 18 For force normal, a similar trend is observed, but with slightly different magnitudes. Spindle speed again shows a strong negative effect where higher speeds result in much lower force normal, indicating reduced lateral resistance during cutting. Feed rate increases force normal gradually from 2 to 6 mm/min, with the steepest rise occurring between mid and high feed levels, due to greater material removal per tooth. Depth of cut has a positive correlation as well, where force normal rises steadily from 40 to 80 μm because a larger engaged area increases the tool's sideways cutting resistance. Hence, for minimizing force normal, the optimal setting remains high spindle speed, low feed rate, and low DOC.

SURFACE QUALITY (RA)

The ANOVA Table 6 presents the statistical analysis of three input parameters on the response. Among these, SS dominates, contributing approximately 89.75% to the overall variation with a P-value of 0.000, indicating an extremely significant effect. FR shows a smaller contribution of 4.88%, but is statistically significant with a P-value of 0.018. Depth of Cut (DOC) contributes just 0.12% with a P-value of 0.656, indicating no statistical significance. The overall model's R-squared value is 94.75%, suggesting the model is very accurate and reliable.

Figure 19 Input parameters are set at Spindle Speed of 15000 rpm, Feed Rate of 5 microns/flute, and Depth of Cut of 40 microns. It can be observed that the surface shows irregular tool marks and deeper feed marks, indicating unstable cutting conditions. The higher roughness is likely due to increased cutting forces, tool vibration, or material adhesion on the cutting edge. Such conditions occur at lower spindle speeds, higher feed rates, or larger depths of cut, which increase chip load and lead to tearing rather than smooth

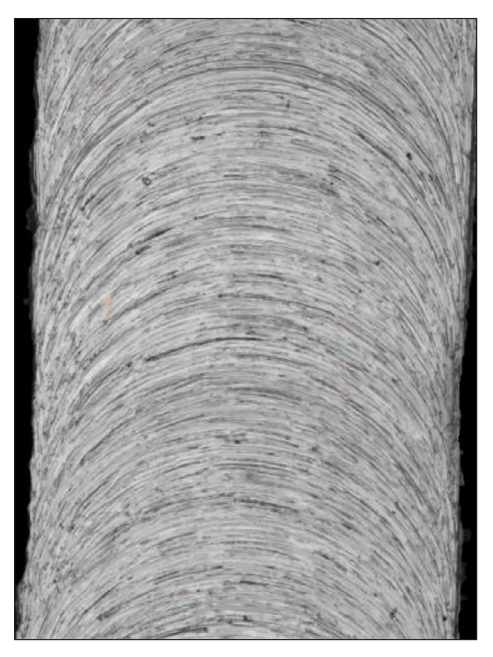


Figure 19. Surface with highest roughness of 0.2076 microns

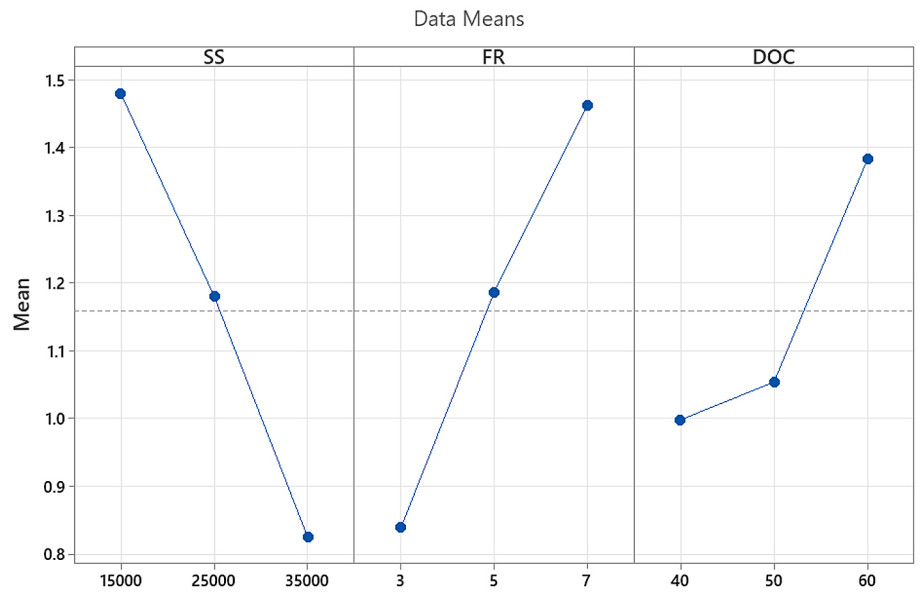


Figure 18. Main effect plot for feed normal

Table 6. ANOVA for surface quality	Table	6. ANO	VA for	surface	quality
---	--------------	---------------	--------	---------	---------

Source	Contribution	Adj SS	Adj MS	F-Value	P-Value
Model	94.75%	0.053279	0.01776	54.15	0
Linear	94.75%	0.053279	0.01776	54.15	0
SS	89.75%	0.050467	0.050467	153.88	0
FR	4.88%	0.002742	0.002742	8.36	0.018
DOC	0.12%	0.00007	0.00007	0.21	0.656
Error	5.25%	0.002952	0.000328		
Total	100.00%				
R-Sq	94.75				

shearing of the aluminium surface. Figure 20 Input parameters are set at Spindle Speed of 35000 rpm, Feed Rate of 3 microns/flute, and Depth of Cut of 60 microns. It can be observed that the surface appears much smoother with finer and more uniform tool marks. The low roughness value reflects stable machining conditions with minimal vibration and controlled material removal. This was achieved under higher spindle speeds, lower feed rates, and shallower depths of cut, where cleaner shearing dominates and material adhesion is minimized. The result is a superior surface finish suitable for precision applications.

Surface quality VS feed rate and spindle speed: Figure 21 and Figure 24, It is found that with an increase in SS, RA decreases, while with an increase in FR, RA increases slightly. For higher SS and lower FR, better surface quality (lower surface roughness) is observed. This is confirmed in the surface plot, which shows that high spindle speed and low

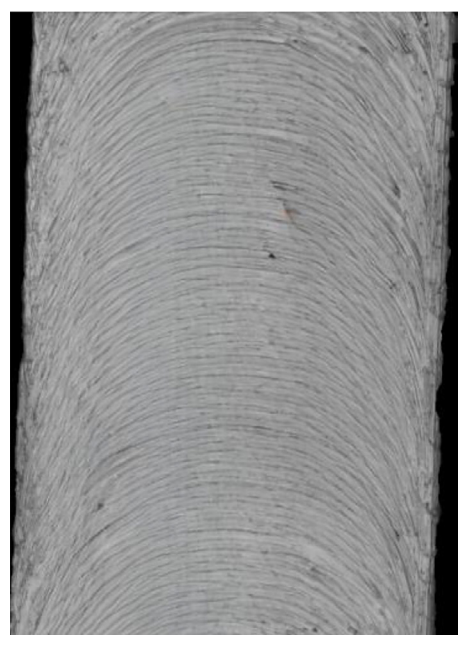


Figure 20. Surface with lowest roughness of 0.0384 microns

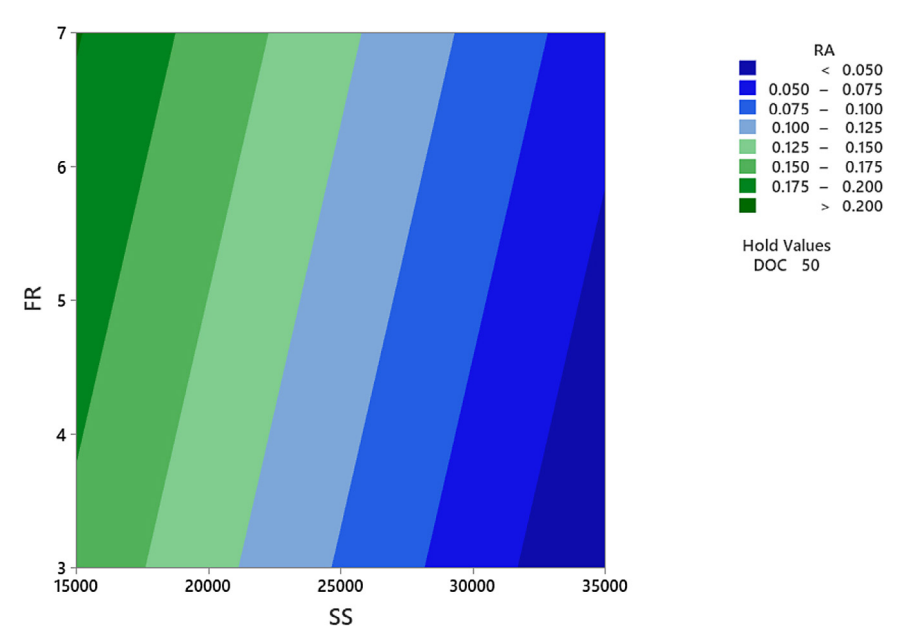


Figure 21. Contour plot for surface roughness VS feed rate and spindle speed

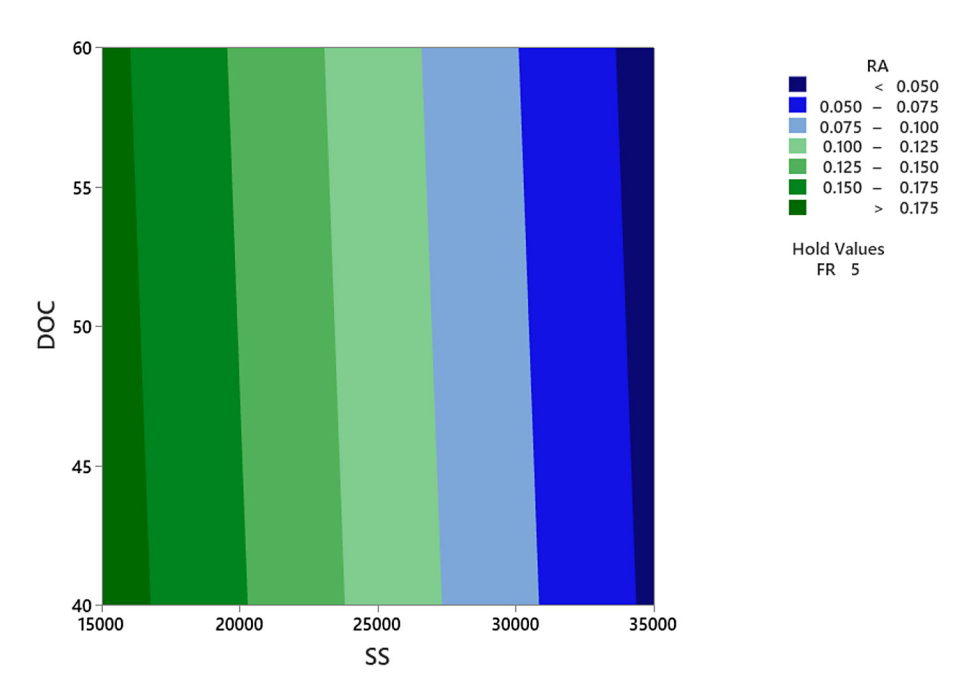


Figure 22. Contour plot for surface roughness VS depth of cut and spindle speed

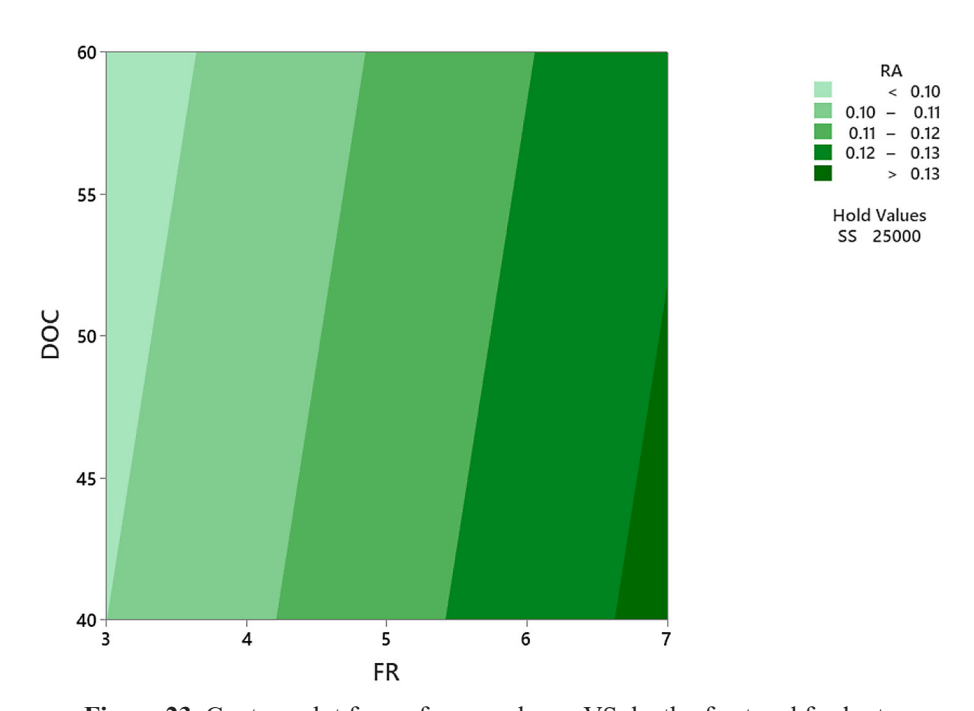


Figure 23. Contour plot for surface roughness VS depth of cut and feed rate

feed rate are favorable for improved surface finish. Surface quality VS depth of cut and spindle speed: Figure 22 and Figure 25, It is found that with an increase in SS, RA decreases, whereas with an increase in DOC, surface roughness increases slightly. For higher SS and lower DOC, better surface quality is observed. This is confirmed in the surface plot, which shows that higher spindle speed and smaller depth of cut produce smoother surfaces. Surface quality VS depth of cut and feed rate:

Figure 23 and Figure 26, It is found that with an increase in FR, RA increases, and with an increase in DOC, RA also increases slightly. For lower FR and lower DOC, better surface quality is observed. This is confirmed in the surface plot, which indicates that low feed surface roughness te and small depth of cut are favorable for producing smoother machined surfaces.

Figure 27, For surface roughness, a similar trend is observed, but with slightly different

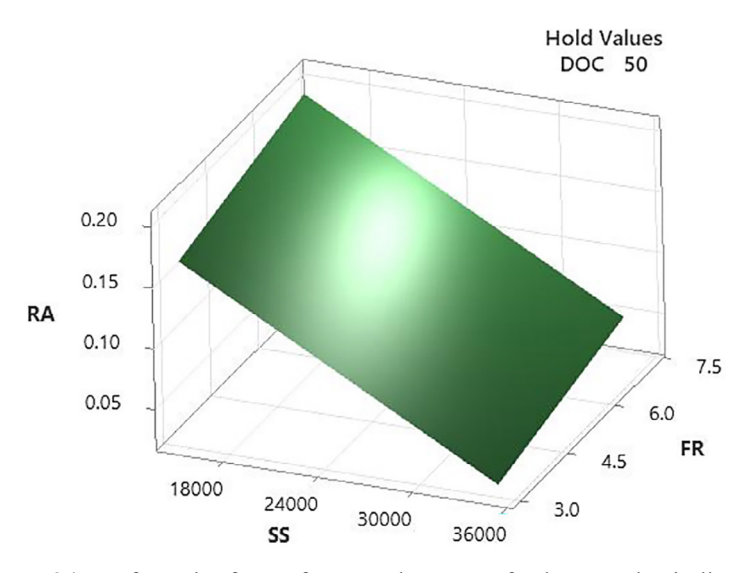


Figure 24. Surface plot for surface roughness VS feed rate and spindle speed

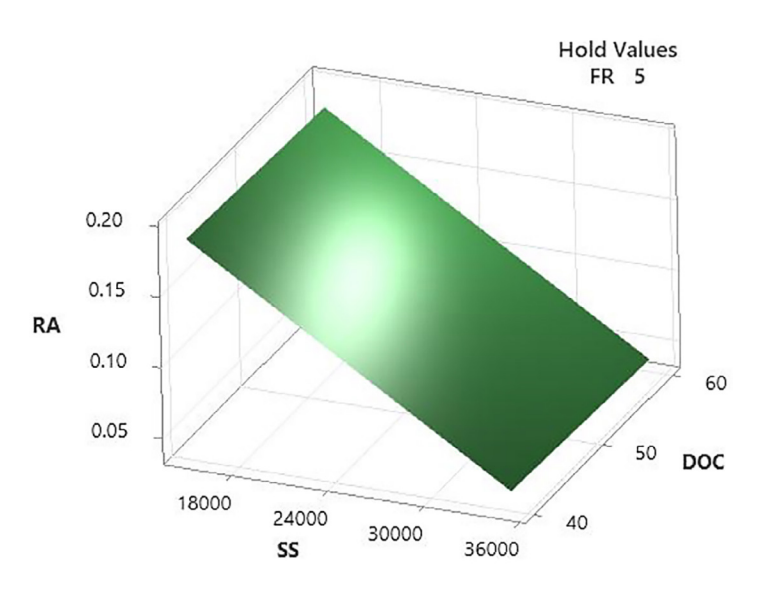


Figure 25. Surface plot for surface roughness VS depth of cut and spindle speed

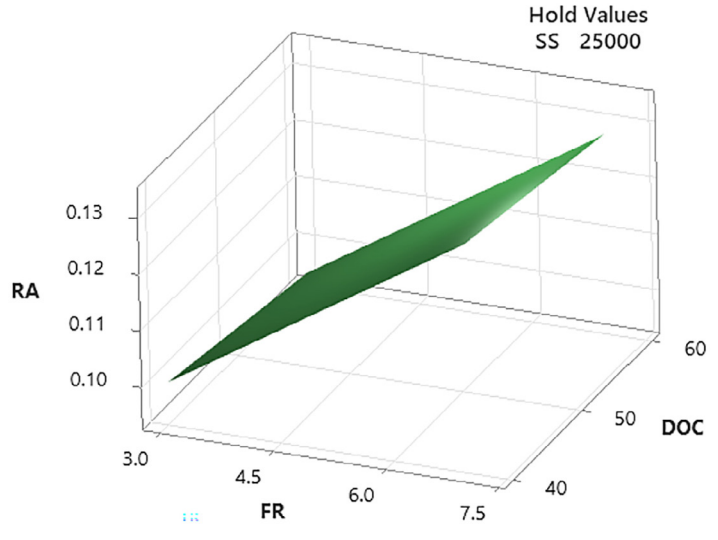


Figure 26. Surface plot for surface roughness VS depth of cut and feed rate

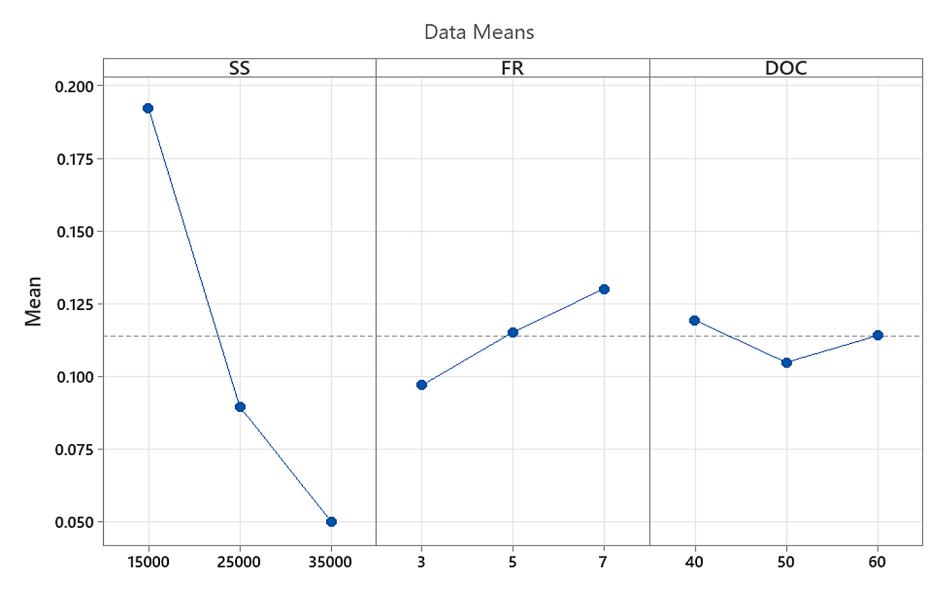


Figure 27. Main effect plot for surface roughness

magnitudes. Spindle speed again shows a strong negative effect, higher speeds result in much lower Ra, indicating reduced lateral resistance during cutting. Feed rate increases surface roughness gradually from 2 to 6 mm/min, with the steepest rise occurring between mid and high feed levels, due to greater material removal per tooth. Depth of cut has a positive correlation as well, where surface roughness rises steadily from 40 to 80 μ m because a larger engaged area increases the tool's sideways cutting resistance. Hence, for minimizing surface roughness, the optimal setting remains high spindle speed, low feed rate, and low DOC.

RESPONSE OPTIMIZATION

A single-objective optimization process generally focuses on improving one response at a time and results in a unique optimal solution. However, in manufacturing processes, multiple response characteristics often need to be optimized simultaneously, which leads to a multi-objective optimization problem and results in multiple optimal solutions. In the present work, the responses considered were surface roughness (Ra), force along feed in the Y-direction (FY), and force along feed in the X-direction (FX), all of which were required to be minimized.

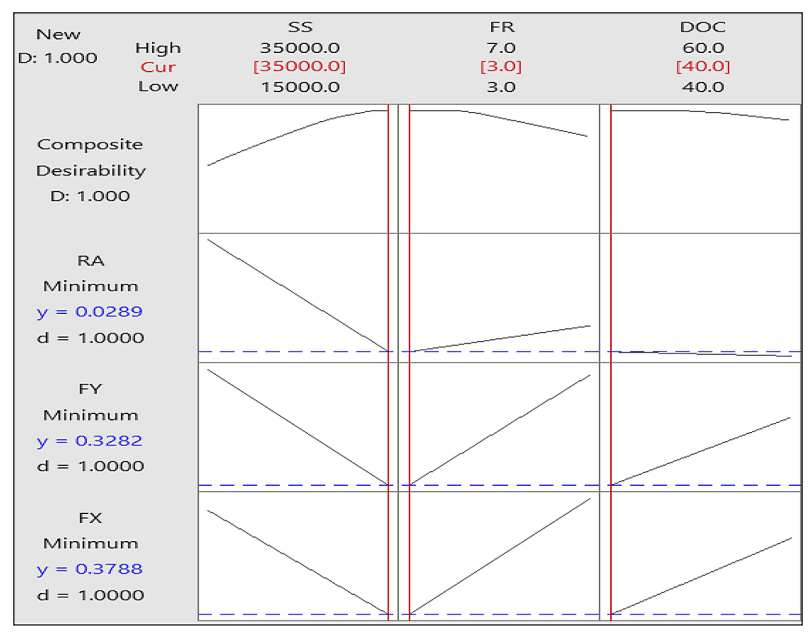


Figure 28. Single-objective optimization graph for best desirability

Table 7. Universal solution of the present multiple optimization problems
--

	Universal solution of the	present multiple optimization problems	
Speed (RPM)	35000	Force along the feed (Fx) (N)	0.3788
Feed (microns/flute)	3	Force normal (Fy) (N)	0.3282
Depth of cut (microns)	0.0289		
	1		

A desirability-based multi-objective optimization technique was employed to obtain a universal solution that balances all objectives. The optimization plot shows the influence of process parameters SS, FR, and DOC on the considered responses. The vertical red lines represent the optimal parameter settings, while the dotted lines denote the response values obtained at those settings. The optimization results revealed that a composite desirability value of 1.000 was achieved, which indicates that the selected solution satisfies all the objectives simultaneously. The optimal combination of process parameters was identified at a spindle speed of 35,000 rpm, feed rate of 3.0 mm/min, and depth of cut of 40 um. At these settings, the predicted response values were $Ra = 0.0289 \mu m$, force normal = 0.3282 N, and force along feed surface roughness = 0.3788 N. Figure 28, The results clearly show that the applied multi-objective optimization approach effectively minimizes the response characteristics simultaneously. The obtained parameter configuration can therefore be considered as the universal solution for the present optimization problem, ensuring superior surface quality and reduced cutting forces (Table 7).

CONCLUSIONS

This research advances the current understanding of parameter-response interactions in aluminium micro-milling by providing quantitative insights into process mechanics and establishing optimized operational windows for superior surface integrity and tool longevity. These results contribute to the development and enabling industries to achieve higher precision, reliability, and productivity in micro-manufacturing

This study demonstrates that uncoated tungsten carbide tools with 7% cobalt binder are a suitable and effective alternative to the conventional 11% cobalt grade for micro-milling of softer materials such as AA6063-T6. The lower cobalt content provided enhanced hardness and wear resistance while avoiding unnecessary toughness, thereby improving tool performance and machining efficiency.

Through an integrated experimental and statistical approach, the fundamental influence of spindle speed, feed rate, and depth of cut on cutting forces and surface roughness was systematically evaluated. This work isolated the intrinsic tool—workpiece interactions and provided ANOVA-driven insights into parameter sensitivities.

In the micro-milling of soft aluminium alloy 6063-T6, spindle speed emerged as the most dominant factor, strongly influencing both surface roughness and cutting forces. ANOVA analysis confirmed this, showing that spindle speed accounted for nearly half of the variations (48–55%), followed by feed rate (25–30%) and depth of cut (15–20%). A higher spindle speed significantly improved machining performance. It reduced cutting forces by 15–25% and enhanced surface finish by up to 40%, mainly due to cleaner shearing and reduced material adhesion. Similarly, lower feed rates minimized chip load, which decreased cutting resistance and ensured more uniform surface textures.

Depth of cut, although less influential, also played a role in machining stability. Shallower cuts reduced tool deflection and vibration, thereby limiting surface defects. The optimal combination of parameters of 35,000 rpm spindle speed, 3.0 μ m/flute feed, and 40 μ m depth of cut resulted in excellent performance, producing a surface roughness of 0.0289 μ m, FY of 0.3282 N, and force along feed of 0.3788 N. Furthermore, tool wear was slower at higher spindle speeds when paired with lower feed rates. This was attributed to reduced cutting forces, which limited micro-chipping of the cutting edge. Overall, controlling spindle speed and feed rate was found to be more effective in enhancing results than simply reducing the depth of cut.

Acknowledgement

I would like to express my sincere gratitude to Dr. Ramesh Singh, Suraj Kumar, Arun Nair, Sashank Shukla and the Machine Tool Lab, Indian Institute of Technology, Bombay for their invaluable support and guidance throughout my project.

REFERENCES

- Shingea A.R., Dabadeb U.A., The effect of process parameters on material removal rate and dimensional variation of channel width in micro milling of aluminium alloy 6063, Procedia Manufacturing, Elsevier, 2018, http://dx.doi.org/10.1016/j. promfg.2018.02.024
- Varghese A., Kulkarni V., Joshi S.S., Tool life stage prediction in micro- milling from force signal analysis using machine learning methods, Journal of Manufacturing Science and Engineering, ASME, 2020, https://doi.org/10.1115/1.4048636
- 3. Baig A., Khan M.A., Jaffery S.H.I., Khan M., Naseer R., Shah I., Petru J., Experimental evaluation of machinability of Monel 400 AlloyDuring high-speed micro milling using various tool coatings, Advances in Science and Technology Research Journal, 2024. http://dx.doi.org/10.12913/22998624/190624
- Muhammad A., Gupta M.K., Mikołajczyk T., Pimenov D. Y., Giasin K., Effect of tool coating and cutting parameters on surface roughness and burr formation during micromilling of Inconel 718, Metals, MDPI, 2021, https://doi.org/10.3390/met11010167
- Davoodi B., Eskandari B., Tool wear mechanisms and multi-response optimization of tool life and volume of material removed in turning of N-155 iron-nickel- base superalloy using RSM, Measurements, Elsevier, 2015, https://doi.org/10.1016/j. measurement.2015.03.006
- Zariatin D.L., Investigation of the micro-milling process of thin-wall features of aluminum alloy 1100, International Journal of Advanced Manufacturing Technology, CrossMark Springers, 2018, https://link.springer.com/article/10.1007%2 Fs00170-017-0514-8
- Vázquez E., Gómez X., Ciurana J., An experimental analysis of process parameters for the milling of micro-channels in biomaterials, Int. J. Mechatronics and Manufacturing Systems, 2012, https://doi. org/10.1504/IJMMS.2012.046145
- 8. Zhang H., Chen L., Sun J., Wang W., Wang Q., An investigation of cobalt phase structure in WC–Co cemented carbides before and after deep cryogenic treatment, Int. Journal of Refractory Metals and Hard Materials, Elsevier, 2015, https://doi.org/10.1016/j.ijrmhm.2015.04.007
- Ucun I., Aslantas K., Bedir F., The performance of DLC-coated and uncoated ultra-fine carbide tools in micromilling of Inconel 718, Precision Engineering, Elsevier, 2015, https://doi.org/10.1016/j. precisioneng.2015.01.002
- Ucun I., Aslantasx K., Bedir F., The effect of minimum quantity lubrication and cryogenic pre-cooling on cutting performance in the micro milling of Inconel 718, J Engineering Manufacture, SAGE, 2015,

- https://doi.org/10.1177/0954405414546144
- 11. Gonçalves M.C.C., Alsters R., CurtisD., M'Saoubid R., Ghadbeigia H., Evolution of surface quality in micromilling Ti-6Al-4V Alloy with increasing machined length, Procedia CIRP, Elsevier, 2024, https://doi.org/10.1016/j.procir.2024.05.040
- 12. Mokhtar M.S.M., Yusoff A.R., Effect of machining parameters on micro-burrs formation of aluminium puncher using high-speed machining process, Journal of Advanced Research in Applied Mechanics, SEMARAK ILMU, 2024, https://doi.org/10.37934/ aram.115.1.4760
- 13. Mokhtar M.S.M., Yusoff A.R., Effect of micromilling parameters on burr formation and surface roughness in aluminum microchannels puncher, Jurnal Tribologi, MYTRIBOS, 2024, https://jurnaltribologi.mytribos.org/v41/JT-41-129-143.pdf
- 14. Özbek N.A., Effects of cryogenic treatment types on the performance of coated tungsten tools in the turning of AISI H11 steel, Journal of Materials Research and Technology, Elsevier, 2020, https://doi.org/10.1016/j.jmrt.2020.03.038
- He Q, Kang X., Wu X., Micro-milling of additively manufactured Al- Si-Mg aluminum alloys, Materials, MDPI, 2024, https://doi.org/10.3390/ma17112668
- Kundiya R., Pawade R., More S., Datir G., Kundiya K., acoustic emission signal correlation with micromachining characteristics of Ti-6Al-4V Alloy, International Journal on Interactive Design and Manufacturing (IJIDeM), Spingers, 2024, http://dx.doi.org/10.1007/s12008-024-01956-2
- 17. Mittal R.K., Kulkarni S.S., Barshilia H., Singh R.K, Machining response and damage evolution of amorphous carbon (WC/a-C) coated tools in high-speed micromilling of Ti-6Al-4V, Journal of Micro and Nano-Manufacturing, ASME, 2020, https://doi.org/10.1115/1.4046192
- Mittal R.K., Singha R.K., Kulkarnia S.S., Kumarb P., Barshiliab H.C., Characterization of anti-abrasion and anti-friction coatings on micromachining response in high-speed micromilling of Ti-6Al-4V, Journal of Manufacturing Processes, Elsevier, 2018.
- S.K. Khare, P. Gulati, J.P. Singh, G.S. Phull, Effect of high-speed machining on surface roughness characteristics Ra, Rq, Rz, E3S Web of Conferences, ICMPC 2023, 2023, https://doi.org/10.1051/e3sconf/202343001271
- 20. S.T. Alam, A.N.M. Amanullah Tomal, M.K. Nayeem, High-speed machining of Ti–6Al–4V: RSM-GA based optimization of surface roughness and MRR. Results in Engineering, Elsevier, 2023, https://doi.org/10.1016/j.rineng.2022.100873
- 21. S. Dehen, E. Segebade, M. Gerstenmeyer, F. Zanger, V. Schulze, Milling parameter and tool wear

- dependent surface quality in micro-milling of brass, Procedia CIRP, Elsevier, 2020
- Z. Liang, P. Gao, X. Wang, S. Li, T. Zhou, J. Xiang, Cutting performance of different coated micro end mills in machining of Ti-6Al-4V, Micromachines, MDPI, 2018, https://doi.org/10.3390/mi9110568
- 23. M.J. Remolina, M.A. Velasco, E. Córdoba, Chip experimental analysis approach obtained by micro-end-milling in (Ti-6Al-4 V) titanium alloy and (7075) aluminium alloy, Journal of King Saud University Engineering Sciences, 2021, https://doi.org/10.1016/j.jksues.2021.04.003
- 24. Rathod V.P., Wankhade S.H. A review on impact of micro-tools on micro-milling outcomes for aluminium alloy. Advances in Science and Technology Research Journal. 2025;19(3):322-340. https://doi.

- org/10.12913/22998624/200007
- 25. Rathod V.P., Wankhade S.H. Comprehensive review of tool treatments and innovations in micro-milling precision and performance. Advances in Science and Technology Research Journal. 2025;19(4):241-257., https://doi.org/10.12913/22998624/200545
- 26. Rathod, V.P., Wankhade, S.H., Kamble, Y.G. (2025). Evaluating the Efficiency of Micro End Mill Tools and Performance Metrics in Micro Milling. *Journal of Mines, Metals and Fuels*, 73(7), 2253–2265. https://doi.org/10.18311/jmmf/2025/49414
- 27. Kamble Y.G., B.R, Rathod V.P., Pantawane P., Wankhade S. Center drill geometry mapping in friction drilling of aluminium 6063 using artificial neural network approach. Advances in Science and Technology Research Journal. 2025;19(11)